Development 135, 75-84 (2008) doi:10.1242/dev.004713

Calcium fluxes in dorsal forerunner cells antagonize β-catenin and alter left-right patterning

Igor Schneider[1], Douglas W. Houston[1], Michael R. Rebagliati[2] and Diane C. Slusarski[1,*]

Establishment of the left-right axis is essential for normal organ morphogenesis and function. Ca^{2+} signaling and cilia function in the zebrafish Kuppfer's Vesicle (KV) have been implicated in laterality. Here we describe an endogenous Ca^{2+} release event in the region of the KV precursors (dorsal forerunner cells, DFCs), prior to KV and cilia formation. Manipulation of Ca^{2+} release to disrupt this early flux does not impact early DFC specification, but results in altered DFC migration or cohesion in the tailbud at somite stages. This leads to disruption of KV formation followed by bilateral expression of asymmetrical genes, and randomized organ laterality. We identify β-catenin inhibition as a Ca^{2+}-signaling target and demonstrate that localized loss of Ca^{2+} within the DFC region or DFC-specific activation of β-catenin is sufficient to alter laterality in zebrafish. We identify a previously unknown DFC-like cell population in *Xenopus* and demonstrate a similar Ca^{2+}-sensitive stage. As in zebrafish, manipulation of Ca^{2+} release results in ectopic nuclear β-catenin and altered laterality. Overall, our data support a conserved early Ca^{2+} requirement in DFC-like cell function in zebrafish and *Xenopus*.

KEY WORDS: Calcium, Laterality, β-catenin, Zebrafish, *Xenopus*, Dorsal forerunner cells

INTRODUCTION

Although vertebrates appear bilaterally symmetrical from the outside, the heart, lungs, liver and gut are carefully positioned across the left-right (LR) axis, and the development of this asymmetry is highly conserved across species. Deviations from the normal internal organ LR arrangement can cause lethality and congenital heart defects (reviewed by Bisgrove et al., 2003). Embryonic organ laterality is preceded by molecular and physiological asymmetries. Asymmetrical H^+/K^+-ATPase expression and gap junctional communication in early cleavage stage *Xenopus* embryos have been proposed to modulate LR signals but may be species specific (reviewed by Levin and Palmer, 2007). During somite stages, asymmetrical gene expression in the lateral plate mesoderm (LPM) becomes apparent. Of note is the left-sided LPM expression of the secreted transforming growth factor-β (TGFβ) related factor *nodal*, a conserved feature in all vertebrate species examined to date (reviewed by Ahmad et al., 2004). Likewise, downstream targets of *nodal*, including *lefty1* and *pitx2*, have conserved asymmetric expression (reviewed by Hamada et al., 2002; Raya and Belmonte, 2006; Wright and Halpern, 2002). Asymmetrical *nodal* expression and LR axis determination in post-gastrula embryos are correlated with the proper structure and function of monocilia located in the embryonic node. Rotation of these monocilia generates a leftward fluid flow in the lumen of the node and is thought to be required for proper LR asymmetry (Hirokawa et al., 2006; Nonaka et al., 1998; Okada et al., 1999). Despite the identification of multiple LR signals, the degree of conservation, as well as the integration and coordination of these independent physiological and molecular signals, is not clearly defined.

In the zebrafish, a structure called Kuppfer's Vesicle (KV) is structurally and functionally homologous to the node, and cilia in the KV are thought to generate critical laterality signals that are propagated to the LPM. The KV is derived from a cluster of non-involuting cells called the dorsal forerunner cells (DFCs), which migrate ahead of the dorsal blastoderm during gastrulation. These cells contribute to both the tailbud and the KV during somite stages (Cooper and D'Amico, 1996; Melby et al., 1996). Furthermore, the DFCs express several genes required for LR patterning and ablation of DFCs disrupts LR patterning (Amack and Yost, 2004; Essner et al., 2005).

Studies in several vertebrate model organisms implicated a requirement for Ca^{2+} signals in LR asymmetry, downstream of fluid flow in the node (Hirokawa et al., 2006) and/or of H^+/K^+ ATPase activity (reviewed by Tabin, 2006). Leftward fluid flow within the node, generated by left-right dynein containing cilia, is thought to stimulate mechanosensory cilia at the node periphery. These cilia contain polycystin-2/PKD-2, a Ca^{2+}-permeable cation channel, and their stimulation triggers elevated intracellular Ca^{2+} levels at the left edge of the mouse node (McGrath et al., 2003). In zebrafish, Ca^{2+} fluxes near the zebrafish KV have been reported and are proposed to be required for normal LR patterning (Sarmah et al., 2005). Additionally, zebrafish embryos mutant for *pkd2* have disrupted expression of laterality markers and organ laterality defects (Schottenfeld et al., 2007). Although the mouse and zebrafish loss-of-function phenotypes are not identical, both models implicate a role for Ca^{2+} release. In an alternative mouse model, the leftward flow of vesicular particles containing *sonic hedgehog* (*shh*) has been postulated to act in a distinct atypical signaling pathway to activate Ca^{2+} on the left side of the node (Tanaka et al., 2005). Elevated Ca^{2+}, in either case, is thought to act via an unknown mechanism, to induce left-sided gene expression (Brennan et al., 2002; Hashimoto et al., 2004; Marques et al., 2004).

In contrast to intracellular Ca^{2+} release, a role for left-sided elevation of extracellular Ca^{2+} has also been proposed. In the chick, differential H^+/K^+ ATPase activity is thought to set up a spatial gradient of extracellular Ca^{2+} by the end of gastrulation, which may be sensed by Notch to activate asymmetrical gene expression (Raya et al., 2004). In zebrafish, disruption of H^+/K^+ ATPase activity also leads to LR asymmetry defects (Kawakami et al., 2005) and disrupts

Departments of [1]Biological Sciences and [2]Anatomy and Cell Biology, University of Iowa, Iowa City, IA 52242, USA.

*Author for correspondence (e-mail: diane-slusarski@uiowa.edu)

Accepted 10 October 2007

KV cilia number and length (Adams et al., 2006). However, in these studies, it was unclear whether intracellular Ca^{2+} was also increased on the left side of the node/KV. Also, in the case of H^+/K^+ ATPase inhibition, *shh* was induced ectopically, an event which could influence laterality.

Thus, several vertebrate models implicate a role for Ca^{2+} signaling in LR asymmetry (Shimeld, 2004), and the data are consistent with a function downstream of H^+/K^+ ATPase or node/KV cilia during somitogenesis. However, it has not been determined whether Ca^{2+} release also has a role in parallel or upstream to KV/node formation and function. In this study, we identified endogenous Ca^{2+} release in the DFC region after the onset of gastrulation, distinct from the events described above and prior to cilia and KV formation. We show that transient inhibition of this Ca^{2+} release results in altered expression of asymmetric markers such as *southpaw*, *lefty1/2* and *pitx2*, randomized placement of organs relative to the LR axis, all preceded by the reduction/loss of KV formation. We further provide several lines of evidence to suggest that the regulation of β-catenin activity is a critical target of Ca^{2+} in the DFCs. First, we show that inhibition of Ca^{2+} release in the DFC region causes a marked increase in nuclear β-catenin and β-catenin transcriptional activity. Second, targeted activation of β-catenin in the DFCs is sufficient to alter laterality. Finally, we describe cells with DFC-like properties in *Xenopus* and establish that the epiboly/gastrula Ca^{2+}-sensitive event is conserved in frogs, as a pulse of Ca^{2+} inhibition in *Xenopus* leads to altered organ laterality and nodal expression as well as ectopic accumulation of β-catenin. Thus, in addition to conserved node-like/cilia development in fish and frog, our results indicate a conserved early Ca^{2+} requirement in LR patterning.

MATERIALS AND METHODS

Embryo manipulation

Zebrafish embryos were collected from natural spawning. Embryos were rinsed with embryo medium (Westerfield, 1995) and staged according to Kimmel et al. (Kimmel et al., 1995). Live embryos were photographed after orienting in 3% methylcellulose. *Xenopus* eggs recovered from females were fertilized in a sperm suspension and maintained in 0.1× MMR.

Pharmacological reagents

Thapsigargin (2.5 μM; Molecular Probes), BODIPY-FL-Thapsigargin (2.5 μM; Molecular Probes), Cyclopiazonic Acid (200 μM; Calbiochem) or Valproic Acid (0.2 mM; Sigma) were diluted in embryo medium. Zebrafish embryos were incubated in thapsigargin for the indicated time and then washed three times in embryo medium. *Xenopus* (stage 11.5) were incubated for 20 minutes in thapsigargin. Xestospongin C (1-2 μM; Calbiochem), was co-injected with Texas Red lineage marker (Molecular Probes) into the yolk of 256- to 512-cell embryos.

Morpholino antisense oligonucleotides (MO)

Control: CCTCTTACCTCAGTTACAATTTATA and Axin1: ACTCATGCTCATAGTGTCCCTGCAC MOs were purchased from Gene Tools, LLC. MO (8 ng) or in vitro transcribed β-catenin 55C RNA (70-100 ng/μl) was co-injected with Texas Red lineage marker (Molecular Probes) into the yolk of 256-512 cell embryos.

LR scoring and whole-mount in situ hybridization (WISH)

Zebrafish cardiac jogging and looping was assessed by light microscopy or by WISH with *nkx2.5*. Gut looping was determined by *foxA3* at 48-52 hpf. *Xenopus* heart and gut orientation was scored under a light microscope (stage 44-46) and laterality was monitored by *xnr1* expression (stage 22-24). For all manipulations, embryos were fixed in 4% paraformaldehyde/1×PBS. Digoxygenin-labeled RNA probes (Roche) were synthesized using linearized templates and the appropriate RNA polymerase. Zebrafish and *Xenopus* hybridizations were done as described (Long et al., 2003; Houston and Wylie, 2005).

TopFlash assay

Zebrafish embryos were injected with either TopFlash or FopFlash as previously described (Park and Moon, 2002), incubated until epiboly stage and treated with thapsigargin or DMSO for 10 minutes at 60% epiboly. After three to five washes with embryo medium, excess medium was removed and embryos were flash frozen at the indicated time (20 or 60 minutes after drug application). Triplicate samples of 15 embryos each were used for TopFlash/FopFlash dual luciferase assays performed following manufacturer instructions (Promega). Luminescence was detected in a Turner Biosystems 20/20n Luminometer.

Immunolocalization

Immunofluorescence was performed according to a standard protocol using anti-acetylated tubulin (Sigma), β-catenin (Sigma) or Ntl (a gift from Dr D. J. Grunwald, University of Utah) followed by fluorescent secondary antibody (Alexa Fluor 488, Molecular Probes) or conjugated anti-horseradish peroxidase (Jackson ImmunoResearch). Confocal image stacks collected at 2 μm intervals were evaluated for nuclear β-catenin.

Syto-11

Syto-11 (Molecular Probes) was diluted in embryo medium to a final concentration of 7.5 μM. Control solution was 2% DMSO in embryo medium. Zebrafish (70% epiboly) and *Xenopus* (stage 11.5) were soaked in Syto-11 for 30 minutes and washed out with excess medium.

Calcium imaging

Zebrafish embryos (one-cell) injected with Fura-2 (dextran-conjugated, Molecular Probes) were oriented with the dorsal shield location noted before collection. The instrumentation for data collection, image analysis software and data manipulations were as described (Slusarski and Corces, 2000).

RESULTS

Localized DFC Ca^{2+} release

As the morphogenetic movements of epiboly progresses, additional cell movements of gastrulation occur, such as involution, convergence and extension, to produce the primary germ layers and the embryonic axis. Ca^{2+}-release activity has been described during epiboly/gastrula stages in both zebrafish and *Xenopus* (Gilland et al., 1999; Wallingford et al., 2001; Webb and Miller, 2006). During epiboly, zebrafish embryos are staged by the extent to which cells have moved over the yolk. At 50% epiboly, the embryonic dorsal shield forms as a thickening on the future dorsal side (Kimmel et al., 1995). The DFCs lie just below the shield and migrate ahead of the shield during gastrulation. At the completion of gastrulation, the DFCs come to lie between the yolk and tailbud and will form the epithelial lining of the KV.

To visualize spatial and temporal changes in live embryos during epiboly/gastrulation, we used the ratiometric Ca^{2+} sensor Fura-2, a reliable measure of intracellular Ca^{2+} (Grynkiewicz et al., 1985). As described in the introduction, Ca^{2+} indicators have been used to investigate the role of Ca^{2+} in LR patterning. Most of the commonly used Ca^{2+} indicators utilize single wavelength excitation and have the potential to interpret signal artifacts as Ca^{2+}-dependent changes. Dual-wavelength detection of Fura-2 has reduced sensitivity to signal artifacts and enables quantitative measurement of Ca^{2+} concentrations. In addition, Fura-2 is less prone to photobleaching (the irreversible destruction of fluorophores) allowing for extended imaging over a developmental time point. Using Fura-2 imaging in zebrafish, we detected localized Ca^{2+} release activity in the shield/DFC region between 60-90% epiboly. In a lateral view of a bright field image, the DFCs resided at the leading edge ahead of the shield region (Fig. 1A, arrow). A single frame of the raw Fura-2 fluorescence of an embryo in a lateral orientation with the shield to the right (Fig. 1B, arrow) and the associated ratio image (Fig. 1C,

arrow) demonstrates localized Ca^{2+} release activity in the region of the DFCs. The transient Ca^{2+} release in the DFC region was most active during 60-70% epiboly and became less active after 75-80% epiboly (see Movie 1 in the supplementary material).

Next, we determined whether a specific developmental process was impacted by experimental suppression of Ca^{2+} release during this time window. To this end, we used thapsigargin, a membrane permeable Ca^{2+}-ATPase inhibitor that prevents the pumping of Ca^{2+} back into the endoplasmic reticulum, resulting in transient increases in cytoplasmic Ca^{2+}, but ultimately causing depletion of internal Ca^{2+} stores (Thastrup et al., 1990; Thastrup et al., 1994). Epiboly stage zebrafish embryos were incubated in thapsigargin at different doses (data not shown) and for different lengths of time (Fig. 1D). The optimal dose was determined to be 2.5 μM thapsigargin for 10 minutes and treatment after 60% epiboly, coinciding with the stages of local Ca^{2+} fluxes observed in the DFC region (see Movie 1 in the supplementary material). Embryos treated at that stage showed normal axial (anterior-posterior and dorsal-ventral) patterning (Fig. 1F,G), but displayed altered LR asymmetry as evaluated by heart jogging (see below; Fig. 1E). Doubling the exposure time did not have any substantial impact upon LR patterning above the optimal treatment (Fig. 1E). Thus, we conclude that brief exposure to thapsigargin after the 60% epiboly stage targets local short-term (or high threshold) signaling, leaving global Ca^{2+} release relatively unperturbed and thereby allowing normal axial patterning. We next explored the nature of the laterality defects and whether DFC differentiation or morphogenesis was affected.

Ca^{2+} inhibition alters organ and molecular LR asymmetry

Heart jogging is one of the first morphological indications of organ LR asymmetry in zebrafish. At 24-30 hpf, the heart tube elongates from the midline and bends, or 'jogs', to the left. To evaluate heart asymmetry embryos can be scored for leftward, rightward or no jog bias (Chen et al., 1997). In untreated, wild-type (wt), embryos, the heart jogged to the left in 95% of the embryos (Fig. 1H and Fig. 2A). In thapsigargin-treated embryos, jogging was randomized, as the heart tube migrated leftward (43%), rightward (25%), or remained in the middle (32%) (Fig. 1H and Fig. 2A-C). A conserved aspect of LR asymmetry among vertebrates is a later morphological looping of the heart, which typically forms a D-loop that places the zebrafish ventricle anterior and to the right of the atrium. In thapsigargin-treated embryos there was concordance between cardiac jogging and looping (see Table S1 in the supplementary material).

If Ca^{2+} inhibition during epiboly disrupts a key LR signal, then the placement of other asymmetrically oriented organs, in addition to the heart, should be altered. This could manifest itself either as heterotaxia (organs adopting laterality independently), or as concordance, which can lead to situs inversus totalis (reversal of all

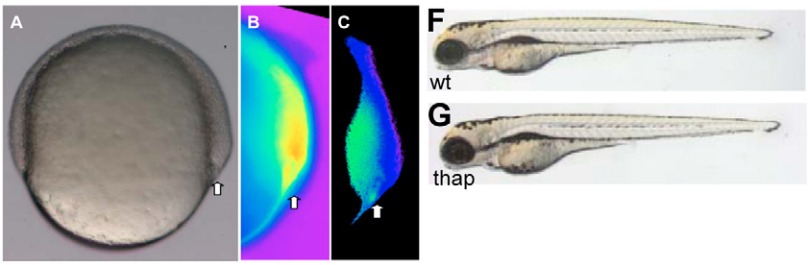

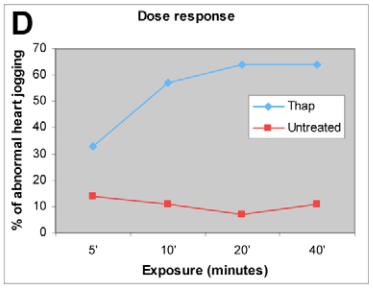

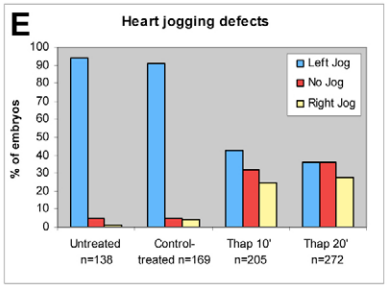

H Organ laterality

	n	Cardiac jogging (%) Left Jog	Right Jog	No Jog
Wild type	225	95	3	2
Control	283	89	5	6
Thap-treated 10'	205	43	25	32
Thap-treated 20'	272	36	28	36

	n	Cardiac looping (%) D-loop	L-loop	No loop
Wild type	138	93	4	3
Control	44	88	5	7
Thap-treated 10'	152	48	27	25
Thap-treated 20'	168	53	27	20

	n	Cardiac jogging	Gut looping (%) Left (WT-like)	Reverse	Symmetric
Control	36	Left jog	100	0	0
	0	Right jog	0	0	0
	0	No jog	0	0	0
Thap-treated 10'	40	Left jog	72	8	20
	21	Right jog	10	76	14
	23	No jog	4	22	74

Fig. 1. Ca^{2+} manipulation impacts organ laterality. (**A-C**) Lateral view, dorsal to the right of 70-80% epiboly stage embryos with arrows indicating the DFC region in (A) bright field image, (B) an individual frame of Fura-2 (380) fluorescence and (C) the corresponding ratiometric image (340/380). The ratio image is converted to pseudo-color with yellow indicating high free intracellular Ca^{2+}. (**D**) Summary plot of thapsigargin exposure vs heart jogging defects. (**E**) Summary of heart jogging defects in wt, control and after 10 and 20 minutes of thapsigargin treatment at 60% epiboly. Lateral view of wt (**F**) and thapsigargin-treated (**G**) embryos. (**H**) Summary of organ laterality defects. Thap, thapsigargin.

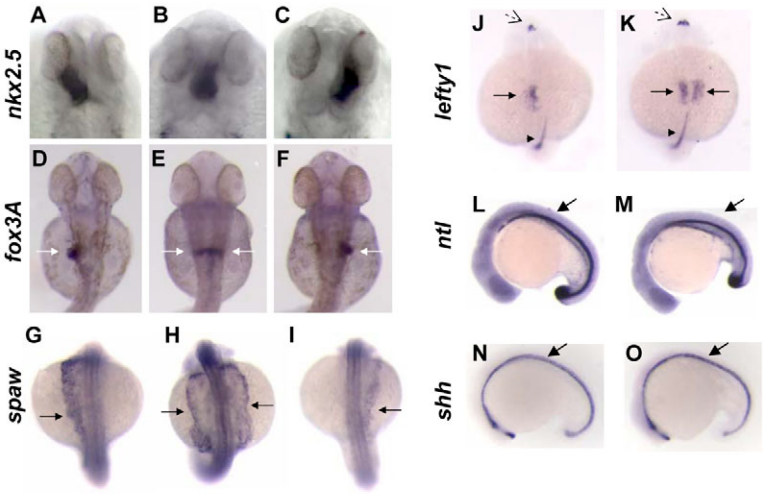

Fig. 2. Thapsigargin treatment disrupts organ laterality and molecular asymmetry. (**A-C**) Dorsal view, 30 hpf, showing *nkx2.5* expression in the heart tube, denoting a left jog in wt (A), and no jog (B) or right jog (C) in thapsigargin-treated embryos. (**D-F**) Dorsal view, 48 hpf, white arrows indicate *foxA3* gut expression in wt (D) and symmetrical (E) or reverse loop (F) in thapsigargin-treated embryos. (**G-I**) Dorsal view, 19-23 somites, arrows indicate left-sided *spaw* expression in (G) wt, and (H) bilateral or (I) right-sided expression in thapsigargin-treated. Dorsal view, 19-23 somites, arrows indicate LPM, dashed arrows indicate brain *lefty1* expression on the left side in (**J**) wt, and (**K**) bilateral in thapsigargin-treated, arrowheads denote *lefty1* expression in the midline. Lateral view of *ntl* expression in (**L**) wt and (**M**) thapsigargin-treated, and *shh* expression in (**N**) wt and (**O**) thapsigargin-treated embryos. (**P**) Summary of asymmetrical marker expression.

P Laterality Markers

			Lateral plate (%)				Dorsal diencephalon (%)			
		n	Left	Right	Bil	Absent	Left	Right	Bil	Absent
	Wild type	46	98	0	2	0	–	–	–	–
spaw	Control	58	98	0	2	0	–	–	–	–
19-23s	Thap-treated	63	11	5	84	0	–	–	–	–
	Wild type	21	86	0	0	14	–	–	–	–
lefty2	Control	33	76	0	0	24	–	–	–	–
19-23s	Thap-treated	37	24	25	40	11	–	–	–	–
	Wild type	57	72	0	0	28	65	0	0	45
lefty1	Control	26	81	0	0	19	81	0	0	19
19-23s	Thap-treated	28	7	14	25	54	7	14	25	54
	Wild type	19	100	0	0	0	32	0	0	68
pitx2c	Control	25	100	0	0	0	48	0	0	52
19-23s	Thap-treated	32	22	16	60	2	0	0	28	72

organ LR asymmetries). Embryos sorted by heart jogging were stained for *foxA3* expression, a larval gut marker (Fig. 1H and Fig. 2D-F) and we found a tight correlation between heart jogging and gut positioning. These results show that organ laterality defects tend to be coordinated in thapsigargin-treated embryos.

To determine whether the randomized organ asymmetry is preceded by alteration of underlying molecular cues, we analyzed several LR markers. The zebrafish *nodal*-related gene *southpaw* (*spaw*) (Long et al., 2003) is the earliest asymmetrical marker in the left LPM during somitogenesis (14-21 hpf). At the 4-6 somite stage, *spaw* expression initiated flanking the KV and this early expression was maintained in thapsigargin-treated embryos (see Fig. S1 in the supplementary material). However, the later asymmetric *spaw* expression in the LPM was dramatically altered in thapsigargin-treated embryos with only a small percentage showing left-sided expression (Fig. 2G-I) compared with wt and control embryos (Fig. 2P). We next investigated markers induced by asymmetric *spaw*, including *lefty1*, *lefty2* and *pitx2c* (reviewed by Ahmad et al., 2004). In wt and control embryos, *lefty1* was expressed in the left anterior LPM (overlapping the prospective heart field) (Fig. 2J), but in treated embryos, expression was predominantly bilateral (Fig. 2K) or reversed. In the developing brain, *pitx2c* and *lefty1* were transiently expressed in the left dorsal diencephalon (Halpern et al., 2003). Wt and control embryos showed left-sided *lefty1* (Fig. 2J), whereas thapsigargin-treated embryos showed altered *lefty1* brain expression (Fig. 2K). Likewise, *lefty2* and *pitx2c* expression was severely disrupted in treated embryos (Fig. 2P and see Fig. S1 in the supplementary material). Thus, thapsigargin treatment disrupts normal asymmetric expression of known molecular cues.

The dorsal midline (notochord and floorplate) is important as a barrier for laterality signals and any gaps in the midline barrier can lead to bilateral *spaw* expression (Bisgrove et al., 2000; Danos and Yost, 1996; Meno et al., 1998). Thus, we evaluated midline integrity in treated embryos. DIC optics in live embryos (Fig. 1G, data not shown) as well as prechordal/notochord expression in the *goosecoid*-GFP transgenic line (Doitsidou et al., 2002) showed normal midline patterning (see Fig. S2 in the supplementary material). At the molecular level, we evaluated three independent notochord and/or floorplate markers (*lefty1*, *ntl* and *shh*) and all three were normal in thapsigargin-treated embryos (Fig. 2J-O). In the case of ntl, we evaluated both RNA (Fig. 2L,M) and protein distribution (see Fig. S2 in the supplementary material). Since *ntl*, *lefty1* and *shh* have essential functions associated with the midline and were expressed, these analyses confirm that brief (10 minute) thapsigargin treatment does not compromise the integrity of dorsal midline tissues.

Analysis of DFC Ca^{2+} source

Thapsigargin treatment of zebrafish embryos yielded dramatic alteration to laterality without alteration to the midline. Typically thapsigargin treatment results in inhibition of Ca^{2+} release. Nevertheless, other studies use thapsigargin to increase Ca^{2+} levels, in particular those that investigate capacitative Ca^{2+} release. To determine whether thapsigargin led to an increase or a loss of the DFC regional Ca^{2+} activity, we performed Fura-2 image analysis in zebrafish embryos at the time of treatment. After application of thapsigargin, we observed suppression of the DFC-regional Ca^{2+} fluxes (see Movie 2 in the supplementary material).

The loss of the DFC Ca^{2+} release activity upon thapsigargin treatment supports a role for intracellular Ca^{2+} in a subset of cells during epiboly.

To substantiate the necessity of DFC regional Ca^{2+}, we tested additional reagents that suppress Ca^{2+} release including: cyclopiazonic acid, a reversible inhibitor of Ca^{2+}-ATPase (Seidler et al., 1989), and valproate, an inhibitor of inositol turnover, targeting the phosphatidylinositol (PI) cycle (Eickholt et al., 2005) as well as Xestospongin C (XeC), a compound that inhibits IP_3-induced Ca^{2+} release (Gafni et al., 1997). All three reagents, cyclopiazonic acid, valproate and XeC, alter heart jogging in treated embryos (data not shown). Embryos treated with valproate and evaluated for asymmetrical gene expression demonstrated altered *lefty* expression (see Fig. S3 in the supplementary material). Taken together, these data support a requirement for Ca^{2+} release in the DFCs for appropriate laterality.

Ca^{2+} inhibition disrupts late aspects of DFC development

Since the DFCs are located in the region of endogenous Ca^{2+} release activity, we investigated DFC specification, migration and endocytic activity after thapsigargin treatment. Several molecular markers are expressed in the DFCs during epiboly (*squint*, *left-right dynein-related-1*/*lrdr1*, *ntl* and *sox17*) (Alexander and Stainier, 1999; Essner et al., 2002; Feldman et al., 1998; Schulte-Merker et al., 1994). We focused on these markers because three of these genes (*lrdr1*, *ntl* and *squint*) are required for proper LR patterning and *sox17* can be used to evaluate morphogenesis. In thapsigargin-treated embryos, robust DFC *sox17* expression was observed at 80% epiboly in a linear domain as opposed to an ovoid shape observed in controls (Fig. 3A,B). *lrdr1* expression at 80% epiboly was similar in wt and thapsigargin-treated embryos (see Fig. S4 in the supplementary material). *squint* expression, a zebrafish *nodal*-related gene, was also maintained (data not shown). DFCs expressed both *ntl* RNA (see Fig. S4 in the supplementary material) and Ntl protein in thapsigargin-treated embryos but the cells did not expand over the yolk as much as in the control (Fig. 3C,D). The presence of early DFC markers supports the fact that Ca^{2+} inhibition does not interfere with the specification of the DFCs. However the compact DFC domain at later epiboly suggests that DFC behavior and or migration may be altered.

Since DFCs are highly endocytic and readily take up vital dyes, such as Syto-11 (Cooper and D'Amico, 1996), we determined whether this aspect of DFC function was affected. Control and thapsigargin-treated embryos incubated in Syto-11 showed similar DFC dye uptake, as visualized by fluorescent microscopy. In thapsigargin-treated embryos, Syto-11 uptake and early migration to the tailbud region was similar to control-treated embryos (see Fig. S4 in the supplementary material). We next monitored DFC migration in vivo by using a GFP transgenic line that marks the DFCs. In the *Dusp6:d2EGFP* transgenic line, EGFP was expressed in a fibroblast growth factor (FGF)-responsive manner in several tissues including the KV and its progenitors (Molina et al., 2007). We directly visualized DFC migration in live embryos from 80% epiboly to four-somite stage (see Movie 3 in the supplementary material). Migration during epiboly was similar in wt and thapsigargin-treated embryos (Fig. 3G,H). By the tailbud to one-somite stage in wt, the DFCs formed a circular cluster at the midline (Fig. 3I) whereas thapsigargin-treated embryos displayed a smaller midline cluster with individual cells scattered nearby (Fig. 3J and see Movie 4 in the supplementary material). By the three- to five-somite stage in wt, the DFCs formed the circular precursor of the KV (Fig. 3K), but in thapsigargin-treated embryos, there was increased dispersal (Fig. 3L).

Evaluation of DFC markers, *lrdr1* and *sox17*, demonstrated a similar migration pattern. DFC migration in thapsigargin-treated embryos appeared the same as in the control during early epiboly but showed increased dispersal of individual cells during somite stages (see Fig. S4 in the supplementary material). Use of another inhibitor, XeC, also resulted in increased dispersal of DFCs, as assayed by the distribution of *sox17* (Fig. 3F). *sox17* is expressed in the endoderm as well as in the DFCs and endodermal expression is similar in control and thapsigargin-treated embryos (Fig. 3A,B). Thus, transient Ca^{2+} inhibition specifically affects the DFCs, and not overall *sox17* expression. These data support the conclusion that inhibition of Ca^{2+} release does not perturb DFC specification, endocytic activity or early migration, but rather is required for later migration or coalescence.

Inhibition of DFC regional Ca^{2+} release suppresses KV formation

The DFCs are KV progenitors (Cooper and D'Amico, 1996; Melby et al., 1996), and thapsigargin treatment resulted in a dramatic loss of a visible KV, with 97% severely reduced or absent (Fig. 4A-D). Thapsigargin-treated embryos also displayed reduced or absent cilia

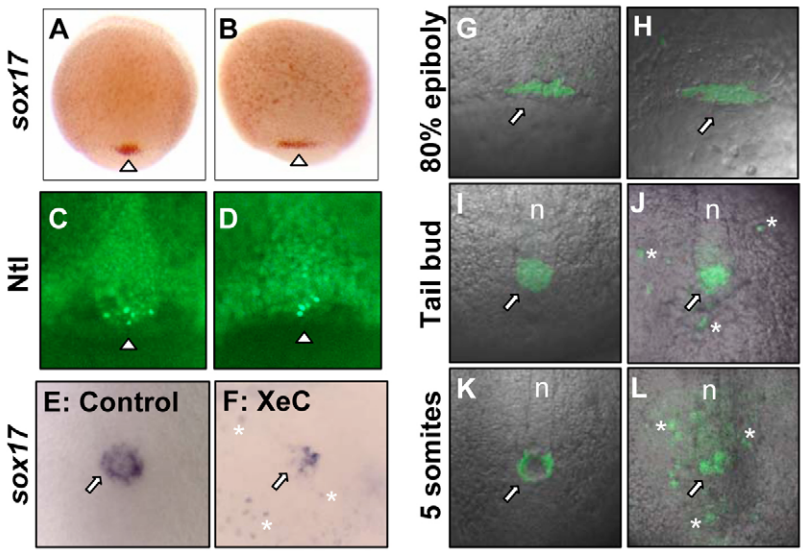

Fig. 3. The DFCs are specified and migrate to the tailbud in thapsigargin-treated embryos. *sox17* expression at 80% epiboly in (**A**) wt and (**B**) thapsigargin-treated embryos. Enriched Ntl protein at 80% epiboly in the DFCs in (**C**) wt and (**D**) thapsigargin-treated embryos; arrowheads note the DFC region. Expression of *sox17* at 4-5 somites in (**E**) wt and (**F**) XeC-treated embryos; asterisks indicate dispersed cells, arrows indicate DFC/KV region. *Tg (Dusp6:d2EGFP)* expression at 80% epiboly in (**G**) untreated and (**H**) thapsigargin-treated embryos; arrows indicate DFCs. *EGFP* expression at tailbud to 1-somite in (**I**) untreated and (**J**) thapsigargin-treated embryos and at 5 somites in (**K**) untreated and (**L**) thapsigargin-treated embryos. XeC, Xestospongin C; n, notochord.

A Morphological and molecular analysis of Kupffer's Vesicle

		Kupffer's Vesicle (%)		
	n	Normal	Reduced	Absent
Wild type	73	100	0	0
Control	59	95	5	0
Thap-treated	67	3	45	52

		Charon (%)		
	n	Normal	Weak signal	No signal
Wild type	36	100	0	0
Control	37	92	8	0
Thap-treated	30	4	66	30

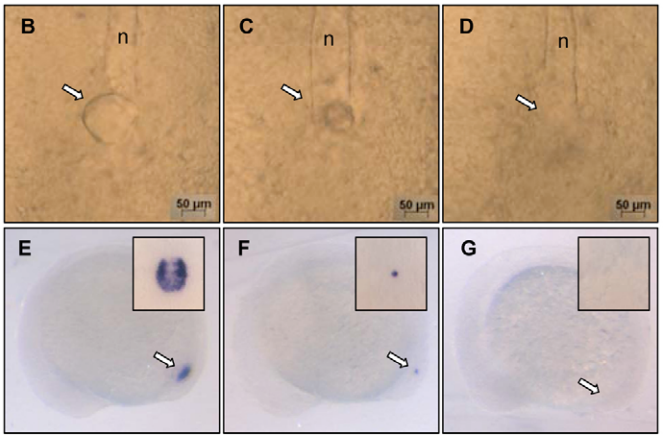

Fig. 4. DFC regional Ca^{2+} is required for KV morphogenesis. (**A**) Summary of KV defects. (**B-D**) Bright field image of wt embryo with normal KV (B) and thapsigargin-treated with reduced (C) and absent (D) KV: dorsal view, 10 somites. Arrows indicate vesicle location; n, notochord. (**E-G**) *charon* expression (arrows) around KV in wt (E) and thapsigargin-treated embryos with reduced (F) and absent (G) signal: lateral view, 10 somites. Insets show dorsal view of *charon* expression. Thap, thapsigargin. Scale bars: 50 μm.

in the KV region (see Fig. S4 in the supplementary material). A subset of KV cells expressed Charon, a Nodal antagonist of the Cer/Dan protein class (Hashimoto et al., 2004). During somite stages, *charon* expression appeared as a horseshoe shape in the tailbud (Fig. 4E) whereas the pattern in thapsigargin-treated embryos was severely reduced (Fig. 4F) or absent (Fig. 4A,G). Thus, loss of the endogenous Ca^{2+} flux during epiboly eliminates *charon* expression and disrupts formation of the KV.

Ca^{2+} signaling negatively controls β-catenin activity

In zebrafish, we previously demonstrated an antagonistic relationship between Ca^{2+} signaling and β-catenin activation (Westfall et al., 2003b). Consequently, we explored the possibility that β-catenin stability may be a target of Ca^{2+} signaling in the DFC region. After 10 minutes of thapsigargin treatment, embryos were washed, cultured until 80% epiboly (50 minutes after treatment) and fixed for immunolocalization. Confocal analysis of β-catenin distribution on both sides of control-treated and wt embryos displayed sporadic cells with nuclear β-catenin in the enveloping layer (EVL) and the yolk syncytial layer (YSL) (Fig. 5A). The EVL, which forms an epithelial monolayer covering the blastoderm, and the YSL, which resides at the blastoderm/yolk margin, are regions where endogenous Ca^{2+} release has previously been detected (Reinhard et al., 1995; Slusarski et al., 1997) and both layers contribute to the DFCs (Cooper and D'Amico, 1996). A marked increase of β-catenin-positive nuclei was observed in thapsigargin-treated embryos (Fig. 5B). Focusing on the DFC-region, there was little or no nuclear β-catenin in wt embryos (Fig. 5C). In contrast, the DFC region of thapsigargin-treated embryos displayed nuclear β-catenin (Fig. 5D). Student's *t*-test analysis of the average number of β-catenin-positive nuclei demonstrated a statistically significant, eightfold increase, in thapsigargin-treated compared with untreated embryos (Fig. 5F). To confirm that ectopic nuclear β-catenin is transcriptionally active, we used TopFlash reporter analyses. TopFlash or FopFlash control vectors were injected into embryos, which were then treated with thapsigargin or control reagent. At 80% epiboly, reporter activity was assayed via relative luminescence units (normalized for *Renilla* control) and TopFlash-injected embryos, but not FopFlash, showed a striking, statistically significant increase after thapsigargin treatment (Fig. 5G). The increased reporter activity at this stage supports the conclusion that thapsigargin treatment leads to transcriptionally active, ectopic β-catenin. Increased TopFlash activity was observed as early as 20 minutes after thapsigargin application (see Fig. S5 in the supplementary material), suggesting a direct response to Ca^{2+} inhibition. For in vivo confirmation of β-catenin activation, we used transgenic embryos expressing destabilized GFP under the control of a β-catenin-responsive promoter, TOPdGFP (Dorsky et al., 2002). In wt embryos at 80% epiboly, there was active Wnt/β-catenin signaling in ventral-lateral domains, reflected by robust TOPdGFP expression, and minimal signal in the DFC region. Thapsigargin treatment induced ectopic GFP expression in the DFCs and flanking regions (see Fig. S5 in the supplementary material).

To determine whether activated β-catenin is sufficient to disrupt LR patterning we targeted a stabilized β-catenin construct [βcat55-C (Pelegri and Maischein, 1998)] to the DFCs, using a procedure developed by Amack and Yost (Amack and Yost, 2004). In this method, reagents injected into the yolk of 256- to 512-cell stage embryos were preferentially taken up by the YSL and DFC progenitors, which maintain cytoplasmic bridges with the yolk cell (DFC-targeting). In our hands, the injections successfully targeted the DFCs with 20-40% efficiency as measured by control GFP RNA or co-injected fluorescent tracer and we assumed a similar efficiency with unlabelled reagents. DFC-directed βcat55-C RNA was sufficient to cause abnormal heart jogging and altered *lefty1/2* expression, whereas control RNA injection had no change in *lefty1/2* expression (Fig. 5H,I). To confirm that the induced defects were due to activated β-catenin at biologically relevant levels, we utilized DFC-targeted *Axin1*-MO (antisense morpholino oligo), a known negative regulator of β-catenin (Heisenberg et al., 2001). *Axin1* knockdown in the DFC region leads to ectopic nuclear β-catenin (Fig. 5E). However, the modest impact of *Axin1* knockdown on *lefty1/2* expression reflects the efficiency of the DFC-targeting; this effect was significant and was sufficient to alter KV formation (see Fig. S5 in the supplementary material). Therefore activated β-catenin in the DFCs is sufficient to alter KV formation and subsequent organ laterality.

To verify that Ca^{2+} activity in the DFC region is critical for KV formation, we utilized DFC targeting of additional Ca^{2+} release inhibitors. KV formation was normal in wt or control-injected (DFC targeting of DMSO) embryos (see Fig. S5 in the supplementary material). Consistent with global thapsigargin treatment, DFC targeting of thapsigargin, or valproate (inositol turnover inhibitor) disrupted KV formation (see Fig. S5 in the supplementary material). Taken together, these data affirm that the defects we observe are primarily due to intracellular Ca^{2+} release inhibition in the DFC region.

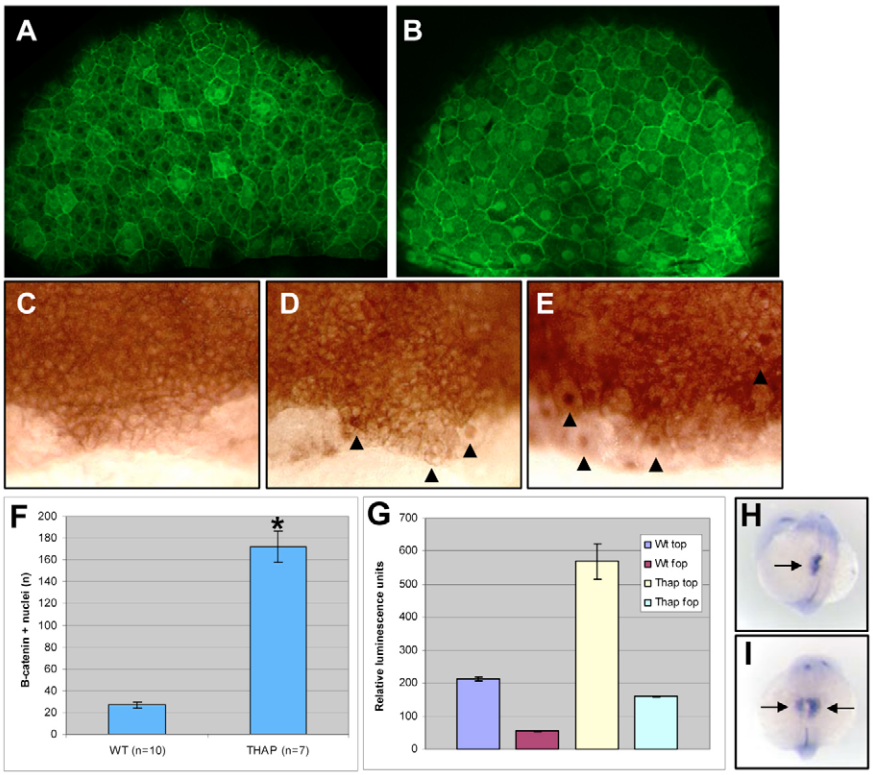

Fig. 5. Ca^{2+} inhibition activates β-catenin and β-catenin is sufficient to alter laterality. Confocal images of β-catenin immunolocalization at 70-80% epiboly in (**A**) wt and (**B**) thapsigargin-treated embryos. HRP staining of β-catenin protein oriented on the DFC region in (**C**) wt, (**D**) thapsigargin-treated and (**E**) DFC-targeted Axin-1 MO-injected embryos; arrowheads indicate β-catenin-positive nuclei. (**F**) Comparison of total nuclear β-catenin in wt and thapsigargin-treated embryos.* indicates *P*-value of 2.5×10^{-5}. (**G**) TopFlash (top) vs. FopFlash (fop) luciferase reporter constructs analyzed for relative luminescence in wt or thapsigargin-treated embryos, normalized to control (*Renilla*) luciferase. Data are means ± s.e. (**H**,**I**) Combined *lefty1* and *lefty2* expression (arrows) in the left LPM and brain in wt (H) and bilateral (I) in DFC-targeted *β-catenin* RNA-injected embryos: dorsal-anterior view, 19-23 somites.

DFC-like cells in *Xenopus*

Our data provide evidence that early Ca^{2+} release in the zebrafish DFC region is necessary for proper KV formation and subsequent LR asymmetry by antagonism of β-catenin. In *Xenopus*, several pieces of evidence suggest that early Ca^{2+} activity near cells with DFC-like properties could be a conserved mechanism for establishing laterality. First, Ca^{2+} release activity has been described near the late organizer region in *Xenopus* gastrula stage embryos (Webb and Miller, 2006). Second, stage 13 *Xenopus* embryos have a cluster of left-right dynein-expressing cells in the dorsal blastopore (Essner et al., 2002) and finally, stage 15 embryos have recently been shown to have motile cilia with left-ward fluid flow in a node-like structure (Schweickert et al., 2007). Thus, we explored the possibility that *Xenopus* embryos have a population of endocytically active cells, which ultimately contribute to the tailbud and form a ciliated structure, analogous to zebrafish DFCs (Cooper and D'Amico, 1996). Syto-11 uptake in late gastrula embryos (stage 11.5) revealed accumulation of labeled cells in the dorsal mesoderm of the tail region of embryos sagittally bisected at stage 14 (Fig. 6A) and stage 17 (neurula) (Fig. 6B). Archenteron roof tissue explants from stage 17 embryos showed Syto-11 staining of the node (Fig. 6C, arrow) and surrounding lateral plate mesoderm. Subsequent immunostaining of the explants for acetylated tubulin showed enrichment of cilia in the node region (Fig. 6D, arrow). These data establish that highly endocytic cells in the late gastrula preferentially contribute to the node region in *Xenopus*.

Ca^{2+} inhibition induces ectopic nuclear β-catenin and laterality defects in *Xenopus*

To determine the extent to which these endocytically active cells share Ca^{2+} sensitivity, we manipulated Ca^{2+} release in *Xenopus*, at a comparable stage of gastrulation (stage 11.5), and using a similar limited exposure as in zebrafish. We visually scored heart and gut laterality after stage 45 (Yost, 1992). Normal organ placement (situs solitus), with the heart ventricle situated on the left side and the outflow tract looping to the right and concomitant counterclockwise coiling of the gut, was observed in 100% of wt and control-treated embryos (Fig. 6E, arrow and M). In thapsigargin-treated embryos, we observed heart-looping and gut-coiling defects (Fig. 6F, arrow and M). Endogenous *Xenopus nodal-related 1* (*xnr1*) expression is detected asymmetrically in the left LPM at stages 22-24 (Fig. 6G,M). Thapsigargin-treated embryos displayed abnormal *xnr1* expression (Fig. 6H,M), showing loss of *xnr1* or bilateral expression in the posterior LPM. Furthermore, thapsigargin treatment was sufficient to induce ectopic nuclear β-catenin on both sides of a stage 13 *Xenopus* embryo compared with the control (Fig. 6I-J and see Fig. S6 in the supplementary material) and as in zebrafish, brief thapsigargin treatment did not alter overall axial anterior-posterior and dorsal-ventral patterning (Fig. 6K,L). In conclusion, these data show that *Xenopus* embryos have endocytically active cells at the late gastrula stage, which contribute to tissues in the tail, similar to zebrafish DFCs. Also, a short pulse of Ca^{2+} inhibition during *Xenopus* gastrulation is sufficient to generate ectopic nuclear β-catenin before node formation and cause laterality defects as observed in zebrafish. These results suggest a conserved Ca^{2+}-sensitive event involving cells with DFC-like properties in LR patterning in non-mammalian vertebrates.

DISCUSSION

Here we report endogenous local Ca^{2+} release in the zebrafish DFC region and show that brief inhibition of Ca^{2+} release during epiboly results in altered DFC coalescence/cohesion, defective KV formation, and disrupted expression of asymmetrical LR signals as well as concordant alteration of organ laterality. We identify β-catenin activity as a candidate target of this Ca^{2+} signaling. These observations link endogenous local Ca^{2+} fluxes and β-catenin regulation to the proper establishment of the KV and subsequent LR asymmetry in the zebrafish embryo. Additionally, we define a DFC-

like cell population in *Xenopus* embryos and demonstrate that these cells share a similar Ca^{2+}-sensitive stage, and exhibit ectopic nuclear β-catenin resulting in altered laterality upon Ca^{2+} perturbation. Our results in both zebrafish and *Xenopus* identify an early Ca^{2+}-sensitive phase relevant to LR patterning that precedes the Ca^{2+} fluxes linked to cilia-driven nodal flow.

Pan-embryonic Ca^{2+} waves during epiboly/gastrula stages are believed to coordinate convergent extension (CE), the lengthening and narrowing of groups of cells, as well as their directed migration to the future dorsal side (Wallingford et al., 2001; Wallingford et al., 2002). Genetic data supports this idea, in that zebrafish homozygous zygotic Wnt-5 mutants (*pipetail*) display CE defects and have reduced Ca^{2+} release frequency (Westfall et al., 2003a). In fact, thapsigargin treatment during 30-50% epiboly resulted in cell movement defects and a shortened anterior-posterior axis (data not shown), consistent with previously described thapsigargin-induced phenotypes (Creton, 2004). However, brief thapsigargin treatment of epiboly/gastrula stage zebrafish and *Xenopus* disrupts laterality without perturbing normal cell movement. Similar laterality defects are generated with additional inhibitors (valproate, to disrupt inositol levels, XeC, to inhibit IP_3-induced Ca^{2+} release and cyclopiazonic acid, to deplete endoplasmic Ca^{2+} stores) and confirm the requirement for early intracellular Ca^{2+} release in KV formation. DFC-targeting of inhibitors supports the conclusion that the Ca^{2+} requirement resides in a small population of cells, as opposed to global signaling over the entire embryo.

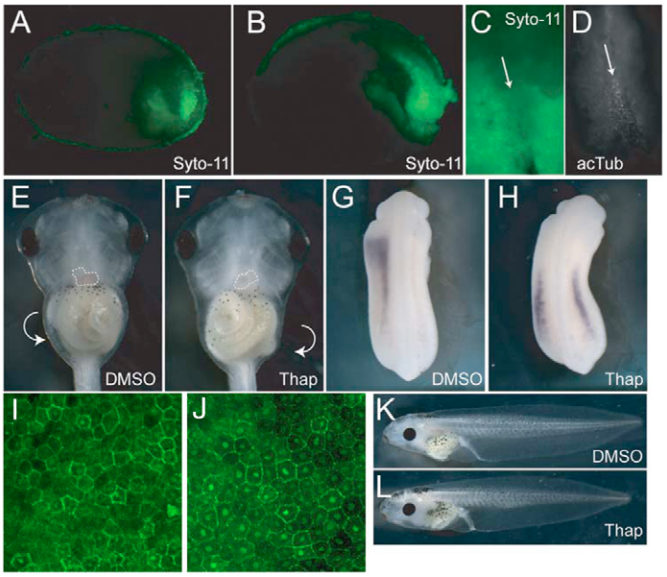

M Organ and *xnr1* Laterality in *Xenopus*

	Organ laterality in *Xenopus* (%)			
	n	Situs solitus	Heterotaxy	Situs inversus
Wild type	34	100	0	0
Control	79	100	0	0
Thap-treated	37	27	60	13

xnr1	Lateral plate (%)				
st 22-24	*n*	Left	Right	Bil	Absent
Wild type	20	100	0	0	0
Control	20	100	0	0	0
Thap-treated	37	24	5	60	11

Fig. 6. *Xenopus* DFC-like cells and Ca^{2+} requirement for laterality. *Xenopus* embryos incubated with Syto-11 at stage 11.5 and sagittally bisected at (**A**) stage 14 and (**B**) stage 17 showing Syto-11-labeled cells enriched in the future tail region. (**C**) Stage 17 archenteron roof explant, showing Syto-11 staining of the node (arrow) and surrounding LPM. (**D**) Explant in C immunostained for acetylated tubulin (acTub), which is enriched in the node region (arrow). (**E**) Ventral view of stage 46 control-treated embryo, showing *situs solitus*, or normal lateral asymmetry. The heart is outlined, showing the left-sided position of the ventricle and right-sided outflow tract. The gut coils counterclockwise, as shown by the arrow. (**F**) Ventral view of a thapsigargin-treated embryo at stage 46, showing an example of *situs inversus*, or reversed laterality. The heart is outlined, showing the right-sided position of the ventricle and left-sided outflow tract. The gut coils clockwise, as shown by the arrow. (**G**) Left-sided *xnr1* expression at stage 22-24 in a DMSO-treated embryo. (**H**) Bilateral *xnr1* expression in a thapsigargin-treated embryo. (**I**,**J**) Lateral view of β-catenin protein localization in control-treated (I) and thapsigargin-treated (J) stage 13 embryos. Note increased number and intensity of nuclear staining. (**K**,**L**) Lateral views of control (K) and thapsigargin-treated (L) embryos, showing normal axial development. (**M**) Summary of *Xenopus* laterality data. Thap, thapsigargin.

Asymmetrical Ca^{2+} levels across the mouse and chick node have been implicated in LR axis determination (McGrath et al., 2003; Raya et al., 2004). The zebrafish KV contains monociliated cells similar to those found in the mouse node and several studies support a link between the node/KV and LR patterning (Brueckner, 2001; Essner et al., 2005; Hashimoto et al., 2004; Supp et al., 1999; Supp et al., 1997). Studies in zebrafish have established a role for inositol polyphosphates, important intracellular second messengers, in LR patterning. Inositol polyphosphate kinases (Ipk) use IP_3 as a template to generate higher inositols (IP_4, IP_5 and IP_6), and play key roles in maintaining Ca^{2+} homeostasis by regulating the concentrations of IP_3 and other inositols (Xia and Yang, 2005). *ipk1* knockdown in zebrafish disrupts laterality, resulting in right-sided or bilateral *spaw* expression (Sarmah et al., 2005). However, *ipk1* is not expressed in the DFCs and in *ipk1* knockdown embryos, KV morphology is normal and cilia are present (Sarmah et al., 2005). Recent work has also postulated a distinct Ca^{2+} requirement in the regulation of KV cilia motility in zebrafish (Shu et al., 2007). These previous studies describe changes in laterality after KV formation. Our findings indicate a novel early role for Ca^{2+} in the DFCs for KV formation. Interestingly in our current study, we found that embryos treated with thapsigargin during tailbud and early somite stages did not have any impact upon KV formation or organ laterality. We used a fluorescent-labeled thapsigargin and noted that upon treatment during epiboly stages, labeled thapsigargin penetrated the YSL and DFC regions (data not shown). Conversely, treatment after tailbud and during somite stages revealed that labeled thapsigargin does not penetrate the region of the embryo where the KV resides. Thus a negative result with thapsigargin treatment at later stages (i.e. somite stages) may be a reflection of failure of the reagent to permeate into the target tissues.

We propose that epiboly stage Ca^{2+} release is required to regulate β-catenin activity in the DFC region. Ca^{2+} inhibition for a discrete time period resulted in a statistically significant increase in nuclear β-catenin and activation of β-catenin transcriptional reporters, including TOPdGFP transgenic embryos and TopFlash assays. In fact, we observe TopFlash activation as early as 20 minutes after addition of thapsigargin, and this activation occurs hours before somitogenesis, KV and cilia formation. This activation is confirmed in the whole embryo by use of the TOPdGFP transgenic line. We also show that DFC endocytic activity and marker gene expression (*ntl*, *lrdr*, *sox17* and *squint*) are maintained in Ca^{2+}-inhibited embryos. Based on in vivo imaging and Syto-11 staining, DFC cell number remained unchanged; however migration within the tailbud region was altered. The labeled cells in the tailbud appear dispersed

and did not coalesce into a KV. This may be due to altered cell adhesion, polarized cell movement or failure to undergo a mesenchymal-to-epithelial transition. All are processes that can be perturbed with altered Wnt signaling or β-catenin levels.

Our data provide evidence for an early Ca^{2+}-dependent cascade that ultimately regulates β-catenin levels and promotes KV formation. Murine Wnt3a has been shown to be necessary in LR coordination, but after the node cilia have formed (Nakaya et al., 2005). Our findings indicate a critical role for Ca^{2+} release and β-catenin activity, specifically in the DFC region before somitogenesis. This may be mediated by Wnt/Ca^{2+} antagonism of Wnt/β-catenin (Slusarski et al., 1997; Torres et al., 1996), however the Wnt/Ca^{2+} ligand is not identified in this study. Since the DFCs do not form a KV in both thapsigargin-treated and *Axin1*-MO injected embryos, we cannot evaluate effects on cilia-dependent laterality cues, but we do observe a loss of charon expression. It should be noted that in *charon* knockdown embryos, the KV remains intact while laterality is altered (M.R., unpublished observations). Conversely, knockdown of Bardet-Biedl Syndrome genes in zebrafish embryos eliminates the morphological aspects of the KV and KV cilia but *charon* is still present (Yen et al., 2006). Furthermore, *charon* knockdown generates a preponderance of embryos with bilateral expression of laterality markers (Hashimoto et al., 2004). Since Ca^{2+} inhibition eliminates *charon* expression, this loss of *charon* can explain the high incidence of bilateral marker gene expression in thapsigargin-treated embryos in the presence of an intact midline.

The dramatic impact upon LR signaling caused by a transient pulse of Ca^{2+} inhibition would suggest a key patterning event and would also be predicted to be shared with other vertebrates. In *Xenopus*, we identified a population of endocytically active cells that ultimately surrounded the putative frog node, thus defining DFC-like properties in another vertebrate. Ca^{2+}-release inhibitors targeting the equivalent developmental stage in *Xenopus*, induced ectopic β-catenin, organ laterality defects and bilateral *nodal* (*Xnr-1*) expression.

In summary, we have identified an early local Ca^{2+} release in the DFC region and show that inhibition of this activity via DFC-targeted injections results in dramatic KV defects. Furthermore, we implicate β-catenin activity as the target of the endogenous DFC Ca^{2+} fluxes and we show that suppression of β-catenin signaling within the DFCs is necessary for appropriate LR patterning in zebrafish and *Xenopus*. Thus, antagonisms between Wnt/Ca^{2+} and Wnt/β-catenin pathways may be crucial not only for dorsal-ventral patterning but for KV morphogenesis and LR asymmetry.

We thank H. Griesbach and T. Westfall for technical assistance and Slusarski lab members for comments on the manuscript. This work was supported by the American Heart Association pre-doctoral fellowship to I.S., Carver Charitable Trust Grants to M.R.R. and D.W.H. and by National Institutes of Health grant CA112369 to D.C.S.

Supplementary material

Supplementary material for this article is available at http://dev.biologists.org/cgi/content/full/135/1/75/DC1

REFERENCES

Adams, D. S., Robinson, K. R., Fukumoto, T., Yuan, S., Albertson, R. C., Yelick, P., Kuo, L., McSweeney, M. and Levin, M. (2006). Early, H^+-V-ATPase-dependent proton flux is necessary for consistent left-right patterning of non-mammalian vertebrates. *Development* **133**, 1657-1671.

Ahmad, N., Long, S. and Rebagliati, M. (2004). A southpaw joins the roster: the role of the zebrafish nodal-related gene southpaw in cardiac LR asymmetry. *Trends Cardiovasc. Med.* **14**, 43-49.

Alexander, J. and Stainier, D. Y. (1999). A molecular pathway leading to endoderm formation in zebrafish. *Curr. Biol.* **9**, 1147-1157.

Amack, J. D. and Yost, H. J. (2004). The T box transcription factor no tail in ciliated cells controls zebrafish left-right asymmetry. *Curr. Biol.* **14**, 685-690.

Bisgrove, B. W., Essner, J. J. and Yost, H. J. (2000). Multiple pathways in the midline regulate concordant brain, heart and gut left-right asymmetry. *Development* **127**, 3567-3579.

Bisgrove, B. W., Morelli, S. H. and Yost, H. J. (2003). Genetics of human laterality disorders: insights from vertebrate model systems. *Annu. Rev. Genomics Hum. Genet.* **4**, 1-32.

Brennan, J., Norris, D. P. and Robertson, E. J. (2002). Nodal activity in the node governs left-right asymmetry. *Genes Dev.* **16**, 2339-2344.

Brueckner, M. (2001). Cilia propel the embryo in the right direction. *Am. J. Med. Genet.* **101**, 339-344.

Chen, J. N., van Eeden, F. J., Warren, K. S., Chin, A., Nusslein-Volhard, C., Haffter, P. and Fishman, M. C. (1997). Left-right pattern of cardiac BMP4 may drive asymmetry of the heart in zebrafish. *Development* **124**, 4373-4382.

Cooper, M. S. and D'Amico, L. A. (1996). A cluster of noninvoluting endocytic cells at the margin of the zebrafish blastoderm marks the site of embryonic shield formation. *Dev. Biol.* **180**, 184-198.

Creton, R. (2004). The calcium pump of the endoplasmic reticulum plays a role in midline signaling during early zebrafish development. *Brain Res. Dev. Brain Res.* **151**, 33-41.

Danos, M. C. and Yost, H. J. (1996). Role of notochord in specification of cardiac left-right orientation in zebrafish and Xenopus. *Dev. Biol.* **177**, 96-103.

Doitsidou, M., Reichman-Fried, M., Stebler, J., Koprunner, M., Dorries, J., Meyer, D., Esguerra, C. V., Leung, T. and Raz, E. (2002). Guidance of primordial germ cell migration by the chemokine SDF-1. *Cell* **111**, 647-659.

Dorsky, R. I., Sheldahl, L. C. and Moon, R. T. (2002). A transgenic Lef1/beta-catenin-dependent reporter is expressed in spatially restricted domains throughout zebrafish development. *Dev. Biol.* **241**, 229-237.

Eickholt, B. J., Towers, G. J., Ryves, W. J., Eikel, D., Adley, K., Ylinen, L. M. J., Chadborn, N. H., Harwood, A. J., Nau, H. and Williams, R. S. B. (2005). Effects of valproic acid derivatives on inositol trisphosphate depletion, teratogenicity, glycogen synthase kinase-3{beta} inhibition, and viral replication: a screening approach for new bipolar disorder drugs derived from the valproic acid core structure. *Mol. Pharmacol.* **67**, 1426-1433.

Essner, J. J., Vogan, K. J., Wagner, M. K., Tabin, C. J., Yost, H. J. and Brueckner, M. (2002). Conserved function for embryonic nodal cilia. *Nature* **418**, 37-38.

Essner, J. J., Amack, J. D., Nyholm, M. K., Harris, E. B. and Yost, H. J. (2005). Kupffer's vesicle is a ciliated organ of asymmetry in the zebrafish embryo that initiates left-right development of the brain, heart and gut. *Development* **132**, 1247-1260.

Feldman, B., Gates, M. A., Egan, E. S., Dougan, S. T., Rennebeck, G., Sirotkin, H. I., Schier, A. F. and Talbot, W. S. (1998). Zebrafish organizer development and germ-layer formation require nodal-related signals. *Nature* **395**, 181-185.

Gafni, J., Munsch, J. A., Lam, T. H., Catlin, M. C., Costa, L. G., Molinski, T. F. and Pessah, I. N. (1997). Xestospongins: potent membrane permeable blockers of the inositol 1,4,5-trisphosphate receptor. *Neuron* **19**, 723-733.

Gilland, E., Miller, A. L., Karplus, E., Baker, R. and Webb, S. E. (1999). Imaging of multicellular large-scale rhythmic calcium waves during zebrafish gastrulation. *Proc. Natl. Acad. Sci. USA* **96**, 157-161.

Grynkiewicz, G., Poenie, M. and Tsien, R. Y. (1985). A new generation of Ca^{2+} indicators with greatly improved fluorescence properties. *J. Biol. Chem.* **260**, 3440-3450.

Halpern, M. E., Liang, J. O. and Gamse, J. T. (2003). Leaning to the left: laterality in the zebrafish forebrain. *Trends Neurosci.* **26**, 308-313.

Hamada, H., Meno, C., Watanabe, D. and Saijoh, Y. (2002). Establishment of vertebrate left-right asymmetry. *Nat. Rev. Genet.* **3**, 103-113.

Hashimoto, H., Rebagliati, M., Ahmad, N., Muraoka, O., Kurokawa, T., Hibi, M. and Suzuki, T. (2004). The Cerberus/Dan-family protein Charon is a negative regulator of Nodal signaling during left-right patterning in zebrafish. *Development* **131**, 1741-1753.

Heisenberg, C. P., Houart, C., Take-uchi, M., Rauch, G. J., Young, N., Coutinho, P., Masai, I., Caneparo, L., Concha, M. L., Geisler, R. et al. (2001). A mutation in the Gsk3-binding domain of zebrafish Masterblind/Axin1 leads to a fate transformation of telencephalon and eyes to diencephalon. *Genes Dev.* **15**, 1427-1434.

Hirokawa, N., Tanaka, Y., Okada, Y. and Takeda, S. (2006). Nodal flow and the generation of left-right asymmetry. *Cell* **125**, 33-45.

Houston, D. W. and Wylie, C. (2005). Maternal Xenopus Zic2 negatively regulates Nodal-related gene expression during anteroposterior patterning. *Development* **132**, 4845-4855.

Kawakami, Y., Raya, A., Raya, R. M., Rodriguez-Esteban, C. and Belmonte, J. C. (2005). Retinoic acid signalling links left-right asymmetric patterning and bilaterally symmetric somitogenesis in the zebrafish embryo. *Nature* **435**, 165-171.

Kimmel, C. B., Ballard, W. W., Kimmel, S. R., Ullmann, B. and Schilling, T. F. (1995). Stages of embryonic development of the zebrafish. *Dev. Dyn.* **203**, 253-310.

Levin, M. and Palmer, A. R. (2007). Left-right patterning from the inside out: widespread evidence for intracellular control. *BioEssays* **29**, 271-287.
Long, S., Ahmad, N. and Rebagliati, M. (2003). The zebrafish nodal-related gene southpaw is required for visceral and diencephalic left-right asymmetry. *Development* **130**, 2303-2316.
Marques, S., Borges, A. C., Silva, A. C., Freitas, S., Cordenonsi, M. and Belo, J. A. (2004). The activity of the Nodal antagonist Cerl-2 in the mouse node is required for correct L/R body axis. *Genes Dev.* **18**, 2342-2347.
McGrath, J., Somlo, S., Makova, S., Tian, X. and Brueckner, M. (2003). Two populations of node monocilia initiate left-right asymmetry in the mouse. *Cell* **114**, 61-73.
Melby, A. E., Warga, R. M. and Kimmel, C. B. (1996). Specification of cell fates at the dorsal margin of the zebrafish gastrula. *Development* **122**, 2225-2237.
Meno, C., Shimono, A., Saijoh, Y., Yashiro, K., Mochida, K., Ohishi, S., Noji, S., Kondoh, H. and Hamada, H. (1998). lefty-1 is required for left-right determination as a regulator of lefty-2 and nodal. *Cell* **94**, 287-297.
Molina, G. A., Watkins, S. C. and Tsang, M. (2007). Generation of FGF reporter transgenic zebrafish and their utility in chemical screens. *BMC Dev. Biol.* **7**, 62.
Nakaya, M. A., Biris, K., Tsukiyama, T., Jaime, S., Rawls, J. A. and Yamaguchi, T. P. (2005). Wnt3alinks left-right determination with segmentation and anteroposterior axis elongation. *Development* **132**, 5425-5436.
Nonaka, S., Tanaka, Y., Okada, Y., Takeda, S., Harada, A., Kanai, Y., Kido, M. and Hirokawa, N. (1998). Randomization of left-right asymmetry due to loss of nodal cilia generating leftward flow of extraembryonic fluid in mice lacking KIF3B motor protein. *Cell* **95**, 829-837.
Okada, Y., Nonaka, S., Tanaka, Y., Saijoh, Y., Hamada, H. and Hirokawa, N. (1999). Abnormal nodal flow precedes situs inversus in iv and inv mice. *Mol. Cell* **4**, 459-468.
Park, M. and Moon, R. T. (2002). The planar cell-polarity gene stbm regulates cell behavior and cell fate in vertebrate embryos. *Nat. Cell Biol.* **4**, 20-25.
Pelegri, F. and Maischein, H. M. (1998). Function of zebrafish beta-catenin and TCF-3 in dorsoventral patterning. *Mech. Dev.* **77**, 63-74.
Raya, A. and Belmonte, J. C. (2006). Left-right asymmetry in the vertebrate embryo: from early information to higher-level integration. *Nat. Rev. Genet.* **7**, 283-293.
Raya, A., Kawakami, Y., Rodriguez-Esteban, C., Ibanes, M., Rasskin-Gutman, D., Rodriguez-Leon, J., Buscher, D., Feijo, J. A. and Izpisua Belmonte, J. C. (2004). Notch activity acts as a sensor for extracellular calcium during vertebrate left-right determination. *Nature* **427**, 121-128.
Reinhard, E., Yokoe, H., Niebling, K. R., Allbritton, N. L., Kuhn, M. A. and Meyer, T. (1995). Localized calcium signals in early zebrafish development. *Dev. Biol.* **170**, 50-61.
Sarmah, B., Latimer, A. J., Appel, B. and Wente, S. R. (2005). Inositol polyphosphates regulate zebrafish left-right asymmetry. *Dev. Cell* **9**, 133-145.
Schottenfeld, J., Sullivan-Brown, J. and Burdine, R. D. (2007). Zebrafish curly up encodes a Pkd2 ortholog that restricts left-side-specific expression of southpaw. *Development* **134**, 1605-1615.
Schulte-Merker, S., van Eeden, F. J., Halpern, M. E., Kimmel, C. B. and Nusslein-Volhard, C. (1994). no tail (ntl) is the zebrafish homologue of the mouse T (Brachyury) gene. *Development* **120**, 1009-1015.
Schweickert, A., Weber, T., Beyer, T., Vick, P., Bogusch, S., Feistel, K. and Blum, M. (2007). Cilia-driven leftward flow determines laterality in Xenopus. *Curr. Biol.* **17**, 60-66.
Seidler, N. W., Jona, I., Vegh, M. and Martonosi, A. (1989). Cyclopiazonic acid is a specific inhibitor of the Ca2+-ATPase of sarcoplasmic reticulum. *J. Biol. Chem.* **264**, 17816-17823.
Shimeld, S. M. (2004). Calcium turns sinister in left-right asymmetry. *Trends Genet.* **20**, 277-280.
Shu, X., Huang, J., Dong, Y., Choi, J., Langenbacher, A. and Chen, J. N. (2007). Na,K-ATPase {alpha}2 and Ncx4a regulate zebrafish left-right patterning. *Development* **134**, 1921-1930.
Slusarski, D. C. and Corces, V. G. (2000). Calcium imaging in cell-cell signaling. In *Developmental Biology Protocols*. Vol. 1 (ed. R. S. Tuan and C. W. Lo), pp. 253-261. Totowa, NJ: Humana Press.
Slusarski, D. C., Yang-Snyder, J., Busa, W. B. and Moon, R. T. (1997). Modulation of embryonic intracellular Ca2+ signaling by Wnt-5A. *Dev. Biol.* **185**, 114-120.
Supp, D. M., Witte, D. P., Potter, S. S. and Brueckner, M. (1997). Mutation of an axonemal dynein affects left-right asymmetry in inversus viscerum mice. *Nature* **389**, 963-966.
Supp, D. M., Brueckner, M., Kuehn, M. R., Witte, D. P., Lowe, L. A., McGrath, J., Corrales, J. and Potter, S. S. (1999). Targeted deletion of the ATP binding domain of left-right dynein confirms its role in specifying development of left-right asymmetries. *Development* **126**, 5495-5504.
Tabin, C. J. (2006). The key to left-right asymmetry. *Cell* **127**, 27-32.
Tanaka, Y., Okada, Y. and Hirokawa, N. (2005). FGF-induced vesicular release of Sonic hedgehog and retinoic acid in leftward nodal flow is critical for left-right determination. *Nature* **435**, 172.
Thastrup, O., Cullen, P. J., Drobak, B. K., Hanley, M. R. and Dawson, A. P. (1990). Thapsigargin, a tumor promoter, discharges intracellular Ca2+ stores by specific inhibition of the endoplasmic reticulum Ca2(+)-ATPase. *Proc. Natl. Acad. Sci. USA* **87**, 2466-2470.
Thastrup, O., Dawson, A. P., Scharff, O., Foder, B., Cullen, P. J., Drobak, B. K., Bjerrum, P. J., Christensen, S. B. and Hanley, M. R. (1994). Thapsigargin, a novel molecular probe for studying intracellular calcium release and storage. 1989. *Agents Actions* **43**, 187-193.
Torres, M., Yang-Snyder, J., Purcell, S., Demarais, A., McGrew, L. and Moon, R. (1996). Activities of the Wnt-1 class of secreted signaling factors are antagonized by the Wnt-5A class and by a dominant negative cadherin in early *Xenopus* development. *J. Cell Biol.* **133**, 1-15.
Wallingford, J. B., Ewald, A. J., Harland, R. M. and Fraser, S. E. (2001). Calcium signaling during convergent extension in Xenopus. *Curr. Biol.* **11**, 652-661.
Wallingford, J. B., Fraser, S. E. and Harland, R. M. (2002). Convergent extension. The molecular control of polarized cell movement during embryonic development. *Dev. Cell* **2**, 695-706.
Webb, S. E. and Miller, A. L. (2006). Ca^{2+} signaling and early embryonic patterning during the blastula and gastrula periods of zebrafish and Xenopus development. *Biochim. Biophys. Acta* **1763**, 1192-1208.
Westerfield, M. (1995). *The Zebrafish Book; A Guide for the Laboratory use of Zebrafish*. Eugene: University of Oregon Press.
Westfall, T. A., Brimeyer, R., Twedt, J., Gladon, J., Olberding, A., Furutani-Seiki, M. and Slusarski, D. C. (2003a). Wnt-5/pipetail functions in vertebrate axis formation as a negative regulator of Wnt/{beta}-catenin activity. *J. Cell Biol.* **162**, 889-898.
Westfall, T. A., Hjertos, B. and Slusarski, D. C. (2003b). Requirement for intracellular calcium modulation in zebrafish dorsal-ventral patterning. *Dev. Biol.* **259**, 380-391.
Wright, C. V. and Halpern, M. E. (2002). Specification of left-right asymmetry. *Results Probl. Cell Differ.* **40**, 96-116.
Xia, H. J. and Yang, G. (2005). Inositol 1,4,5-trisphosphate 3-kinases: functions and regulations. *Cell Res.* **15**, 83-91.
Yen, H. J., Tayeh, M. K., Mullins, R. F., Stone, E. M., Sheffield, V. C. and Slusarski, D. C. (2006). Bardet-Biedl syndrome genes are important in retrograde intracellular trafficking and Kupffer's vesicle cilia function. *Hum. Mol. Genet.* **15**, 667-677.
Yost, H. J. (1992). Regulation of vertebrate left-right asymmetries by extracellular matrix. *Nature* **357**, 158-161.

Table S1. Heart jogging vs looping (%)

	Jogging	*n*	D-loop	L-loop	No loop
Wild type	Left jog	160	99	0	1
	Right jog	2	0	50	50
	No jog	8	12	50	38
Control	Left jog	190	99	0	1
	Right jog	8	25	50	25
	No jog	10	50	20	30
Thapsigargin-treated	Left jog	45	80	6	14
	Right jog	27	22	63	15
	No jog	27	30	22	48